Tuijin Jishu/Journal of Propulsion Technology
ISSN: 1001-4055
Vol. 45 No. 2 (2024)

Comparative Analysis of Lithium-Ion Cell Performance Using Different Cathode Materials Under Drive Cycle Simulations

Srinivas Mallimoggala[1], K Rama Devi[2]
ECE Dept., University College of Engineering, JNTUK Kakinada[1,2]

Abstract: **-** The research presents a comprehensive investigation into the performance characteristics of lithium-ion cells utilizing different cathode materials, namely Lithium Cobalt Oxide (LCO), Lithium Manganese Oxide (LMO), Nickel Manganese Cobalt Oxide with a ratio of 1:1:1 (NMC 111), Nickel Manganese Cobalt Oxide with a ratio of 8:1:1 (NMC 811), and Lithium Nickel Cobalt Aluminum Oxide (NCA). Drive cycle simulations are conducted using the COMSOL Multiphysics software to analyze various cell parameters, including boundary electric potential, current, cell voltage, state of charge (SOC), and electrode SOC's. A comparative study is performed to identify the materials yielding the highest and lowest values for each output parameter. The results of this study offer valuable insights into the performance characteristics of different lithium-ion cell materials under varying operating conditions, thereby aiding in the selection and optimization of suitable materials for specific applications.

Keywords*: Lithium-ion cells, Cathode materials, LCO, LMO, NMC, NCA, Drive cycle, COMSOL Multiphysics*

1. Introduction

The rapid advancement of lithium-ion battery technology has revolutionized the field of energy storage, enabling diverse applications ranging from portable electronics to electric vehicles and grid energy storage systems. The performance of lithium-ion batteries is influenced by various factors, including cell materials, which play a crucial role in determining key performance indicators such as boundary electric potential, cell voltage, polarization, and cell currents [8]. Understanding the performance characteristics of different cell materials is essential for optimizing battery performance and ensuring reliable operation in various applications.

In this research paper, we present a comprehensive comparative analysis of lithium-ion battery materials to assess their suitability for performance optimization in energy storage systems. The study utilizes a 1-D electrochemical model to simulate charge-discharge cycles across various cell materials and analyze key performance indicators [2]. The results of the simulation provide valuable insights into the performance characteristics of different cell materials and their implications for energy storage system design and optimization. The comparative analysis focuses on evaluating the following key performance indicators:

1. Boundary Electric Potential and Cell Voltage: Boundary electric potential refers to the voltage difference between the electrolyte and the electrodes at the interface within a lithium-ion battery. This parameter plays a crucial role in determining the battery's voltage output, energy density, power capabilities, and overall electrochemical performance [4,8,10]. Understanding the dynamics and implications of boundary electric potential variations is essential for optimizing battery design, enhancing performance, and ensuring application suitability across diverse operational environments.
2. Polarization: Polarization in the context of lithium-ion batteries refers to the deviation of voltage from the equilibrium potential during charge and discharge processes. It is a complex phenomenon arising from various factors within the battery system, including resistance encountered by ions as they migrate through the electrolyte and electrode materials, as well as kinetic limitations at the electrode-electrolyte interface [7,11,13-15]. Positive and Negative Electrode State of Charge (SOC): The study examines the positive and negative electrode SOC to

evaluate the availability of stored energy within the electrodes and its implications for energy output and performance [1,4,8].

3. Cell Currents: Cell current in lithium-ion batteries refers to the flow of electric charge (measured in amperes, or amps) within the battery during charge and discharge processes. It represents the rate at which electrons are transferred between the electrodes through the external circuit, and it directly influences the battery's power output, charging/discharging rate, and overall performance [3,4,12].

2. Model structure

The model utilized commercial finite-element software, specifically COMSOL Multiphysics 6.0, to implement a single-dimensional model of a lithium-ion battery [2]. The sample model of drive cycle is taken from application libraries in COMSOL Multiphysics simulation software. The Lithium-ion battery (li-ion) physics interface was employed to simulate the electrochemical behavior of the battery and analyze performance metrics including state of charge (SOC) [1,4,8], electrolyte potential, electrode potential, polarization, electrode salt concentration, cell current, and cell and electrode voltages for five types of cell materials.

Fig 1a: Cell geometry of 1-D lithium-ion battery porous electrode 1

Fig 1b: Cell geometry of 1-D lithium-ion battery Separator

Fig 1c: Cell geometry of 1-D lithium-ion battery porous electrode.

3. Parameters of the cell

Battery capacity (Q_B) and initial cell voltage (Ecell_init) are taken based on the simulations performed in lithium battery designer are Listed in the table 1.

Table 1: Cell material parameters.

	LCO		LMO		NCA		NMC 111		NMC 811		
Cell positive electrode thickness	Cell negative electrode thickness	Cell capacity	Cell negative electrode thickness	Cell capacity	Cell negative electrode thickness	Cell capacity	Cell negative electrode thickness	Cell capacity	Cell negative electrode thickness	Cell capacity	cell voltage
45 µm	47.6 µm	3.31 A-h	28 µm	2.75 A-h	53.5 µm	3.42 A-h	72.8 µm	3.69 A-h	57.9 µm	3.5 A-h	4.2 V
50 µm	52.9 µm	3.41 A-h	31.1 µm	2.86 A-h	59.4 µm	3.52 A-h	80.9 µm	3.77 A-h	64.3 µm	3.59 A-h	4.2 V
55 µm	58.2 µm	3.5 A-h	34.2 µm	2.97 A-h	65.4 µm	3.6 A-h	89 µm	3.84 A-h	70.7 µm	3.67 A-h	4.2 V
60 µm	63.5 µm	3.58 A-h	37.4 µm	3.06 A-h	71.3 µm	3.67 A-h	97.1 µm	3.9 A-h	77.1 µm	3.74 A-h	4.2 V
65 µm	68.8 µm	3.64 A-h	40.5 µm	3.15 A-h	77.3 µm	3.74 A-h	105 µm	3.95 A-h	83.6 µm	3.8 A-h	4.2 V
70 µm	74.1 µm	3.7 A-h	43.6 µm	3.22 A-h	83.2 µm	3.79 A-h	113 µm	4 A-h	90 µm	3.85 A-h	4.2 V
75 µm	79.4 µm	3.76 A-h	46.7 µm	3.29 A-h	89.1 µm	3.84 A-h	121 µm	4.04 A-h	96.4 µm	3.9 A-h	4.2 V
80 µm	84.7 µm	3.81 A-h	49.8 µm	3.36 A-h	95.1 µm	3.89 A-h	129 µm	4.07 A-h	103 µm	3.94 A-h	4.2 V

The Lithium-ion Battery Interface is crucial for understanding and modeling various aspects of lithium-ion batteries. It encompasses the current and mass balances in the electrolyte and electrodes, as well as the electrochemical reactions occurring within the battery [2]

The interface defines key parameters and equations for analyzing lithium-ion battery behavior. It considers the electrolyte as a quiescent 1:1 binary solution containing lithium cations (Li^+) and anions (An^-). The interface solves for five dependent variables: electric potential (f_s), electrolyte potential (f_l), potential losses due to a resistive film on electrode particles ($Df_{s,film}$), lithium concentration in electrode particles (c_s), and electrolyte salt concentration (c_l).

$$\nabla.\left(-\sigma_l\nabla\phi_l + \frac{2\sigma_l RT}{F}\left(1+\frac{\partial \ln f}{\partial \ln c_l}\right)(1-t_+)\nabla \ln c_l\right)$$

$$= i_{tot} + Q_l\varepsilon_l\frac{\partial c_l}{\partial t} + \nabla.(-\varepsilon_l D_l \nabla c_l)$$

$$= R_l - \left(\frac{i_{tot}+Q_l}{F}\right)t_+$$

Electrochemical reactions occur at the surface of solid spherical particles in electrodes, described as insertion reactions [2]. The concentration of reaction sites (Θs) and state-of-charge variable (soc) are important parameters. The mass balance of Li in solid particles is described, considering diffusion to and from the surface.

$$c_{\Theta_s} = c_{s,max} - c_s$$

$$soc = \frac{c_s}{c_{s,max}}$$

Boundary conditions are set for solid particle surfaces, accounting for lithium flux caused by electrochemical reactions [2]. Stoichiometric coefficients and the number of electrons involved in electrode reactions are defined, particularly for lithium insertion reactions. The equation goes as:

$$\sum_{\text{ox}} \nu_{\text{ox}} S_{\text{ox}} + ne^- \Leftrightarrow \sum_{\text{red}} \nu_{\text{red}} S_{\text{red}}$$

In porous electrodes, the total charge transfer current density i_{tot} is determined, along with additional reaction sources contributing to species source [2]. At the particle surface, equations account for scaling factors and solid phase diffusion coefficients.

$$i_{\text{tot}} = \sum A_{\text{v,m}} i_{loc,m}$$

For modeling a resistive film (SEI), an extra solution variable for potential variation over the film is introduced, with corresponding governing equations.

$$\Delta\phi_{s,\text{film}} = i_{\text{tot}} R_{\text{film}}$$

Overall, the interface provides a comprehensive framework for analyzing lithium-ion battery behavior, considering various physical and electrochemical phenomena [2].

$$\eta_m = \phi_s - \Delta\phi_{s,\text{film}} - \phi_l - E_{eq,m}$$

Table 2: Material type and its electrode thickness.

	45	50	55	65	70	75	80
LCO	✓	✓	✓	✓	✓	✓	-
LMO	✓	✓	✓	✓	✓	✓	✓
NCA	✓	✓	✓	✓	✓	✓	✓
NMC 111	✓	✓	✓	-	-	-	-
NMC 811	✓	✓	✓	✓	✓	-	-

4. Results

The electrochemical model proposed for a 1-D lithium-ion battery during drive cycles underwent simulation to analyze charge-discharge cycles across various cell materials. This study aimed to investigate key performance indicators such as boundary electric potential, cell voltage, polarization, state of charge (SOC) for both the cell and electrodes, and cell current. The comparative analysis provided valuable insights into the suitability of different cell materials for various applications.

1. Boundary Electric Potential and Cell Voltage: The results revealed in figure 2 that LCO (Lithium Cobalt Oxide) exhibited the highest boundary electric potential and cell voltage among the materials tested. This finding indicates the potential for LCO to deliver high voltage output, making it promising for applications requiring elevated power levels. Conversely, LMO (Lithium Manganese Oxide) demonstrated the lowest boundary electric potential and cell voltage. This suggests that LMO may face limitations in providing high voltage output, which could impact its suitability for certain applications.

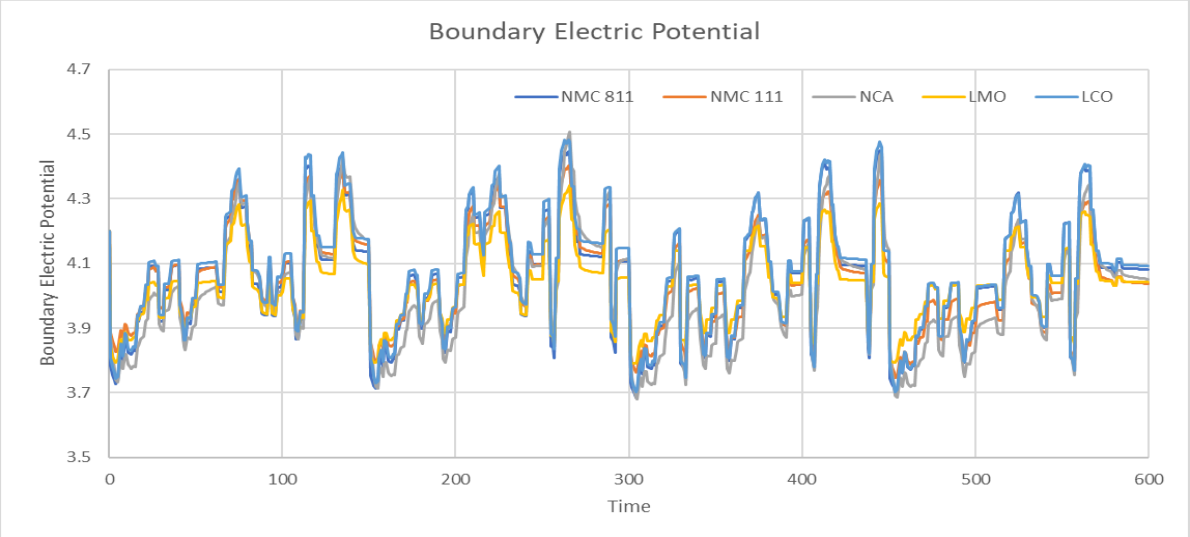

Figure 2: Comparison of Boundary electric potential with all cell materials.

2. Polarization: The analysis showed in the figure 3 that LCO exhibited higher polarization compared to LMO. Polarization refers to the resistance to ion diffusion and charge transfer within the battery system. The higher polarization observed in LCO indicates potential challenges in these processes, which could affect the overall performance of the cell. This finding underscores the importance of considering polarization when assessing the suitability of cell materials for specific applications.

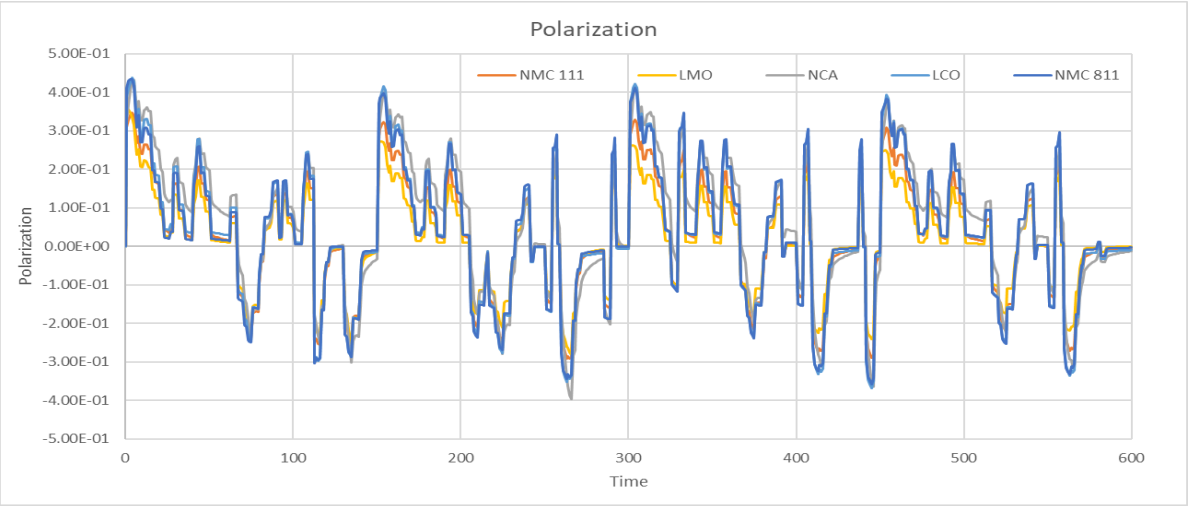

Figure 3: Comparison of polarization with all materials

3. Positive Electrode SOC: In the Figure 4 LCO demonstrated the highest positive electrode SOC among all the cell materials tested. This indicates that a significant portion of lithium ions within the positive electrode material are in a charged state compared to the maximum possible capacity. A high positive electrode SOC is desirable for applications requiring sustained energy output and performance.

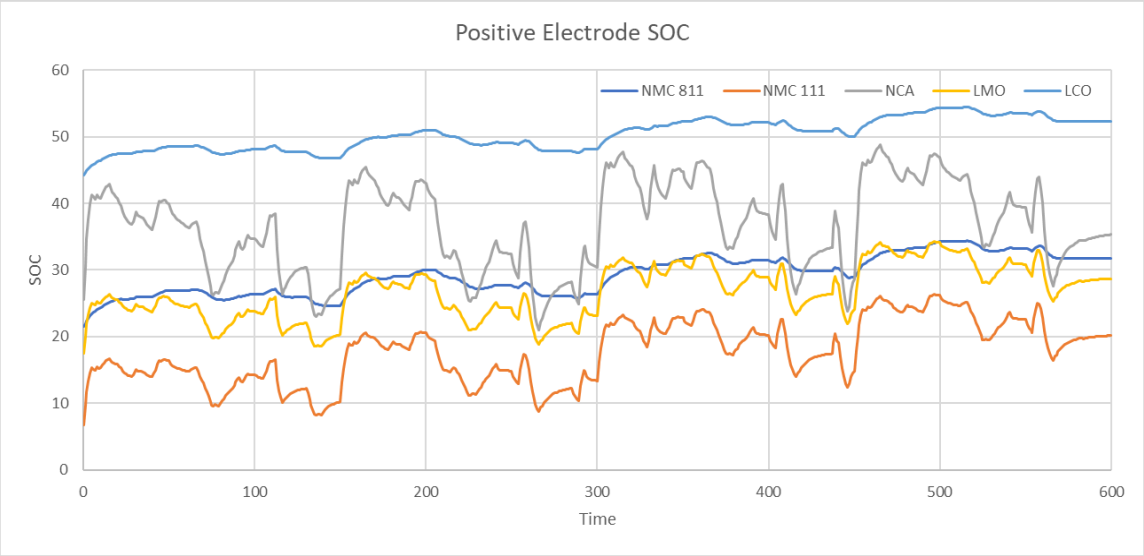

Figure 4: Comparison of positive electrode SOC with all cell the materials.

4. Negative Electrode SOC: The results in the figure 5 showed that NMC 811 (Nickel Manganese Cobalt Oxide) exhibited the highest negative electrode SOC compared to other cell materials. This suggests that a significant portion of lithium ions within the negative electrode material are intercalated or stored compared to the maximum possible capacity. A high negative electrode SOC is advantageous for applications demanding rapid energy release and high-power output.

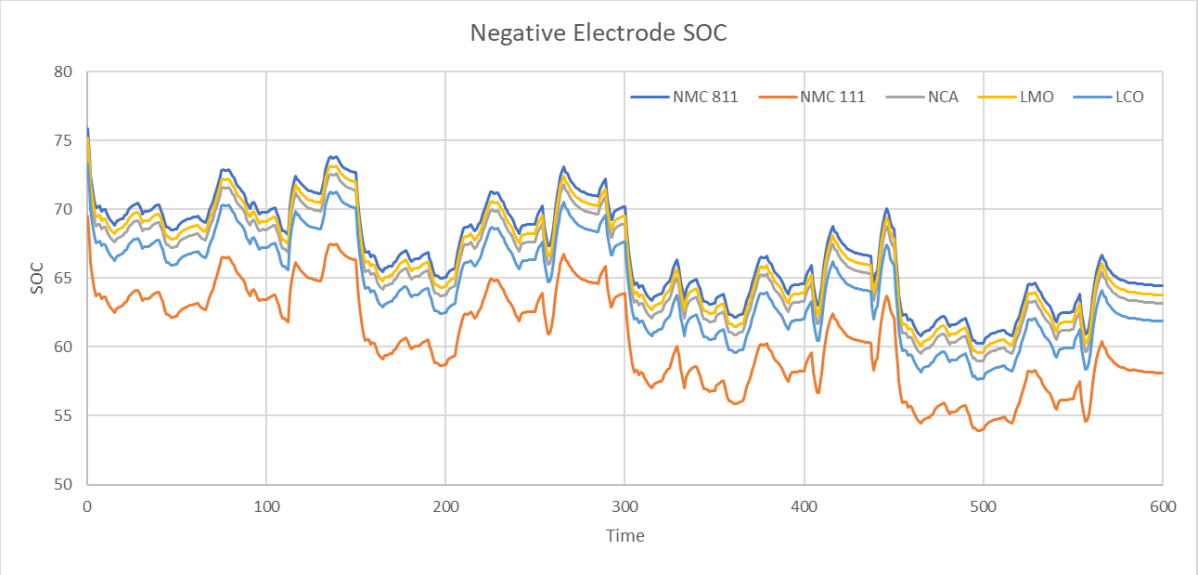

Figure 5: Comparison of negative electrode SOC with all the cell materials.

5. Average Electrode SOC: In figure 6 NMC 811 demonstrated higher average positive electrode SOC, while in figure 7 LCO offered higher average negative electrode SOC. These values represent the average state of charge of the electrodes over a specified period of time or operation cycle. The findings highlight the importance

of considering the average electrode SOC in assessing the overall performance and suitability of cell materials for specific applications.

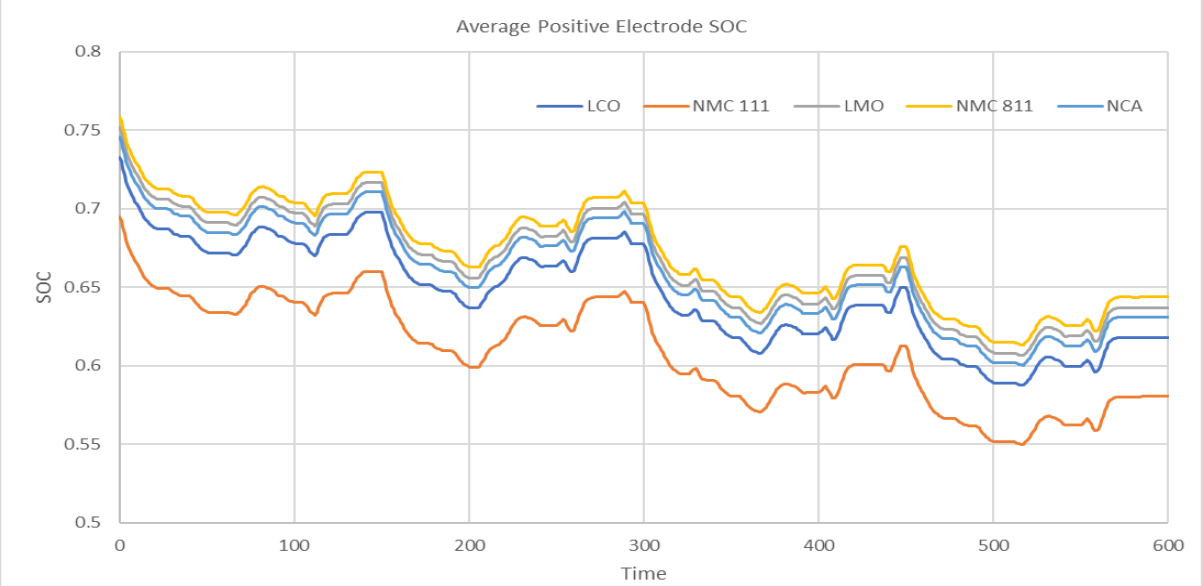

Figure 6: Comparison of Average positive electrode SOC with all the cell materials.

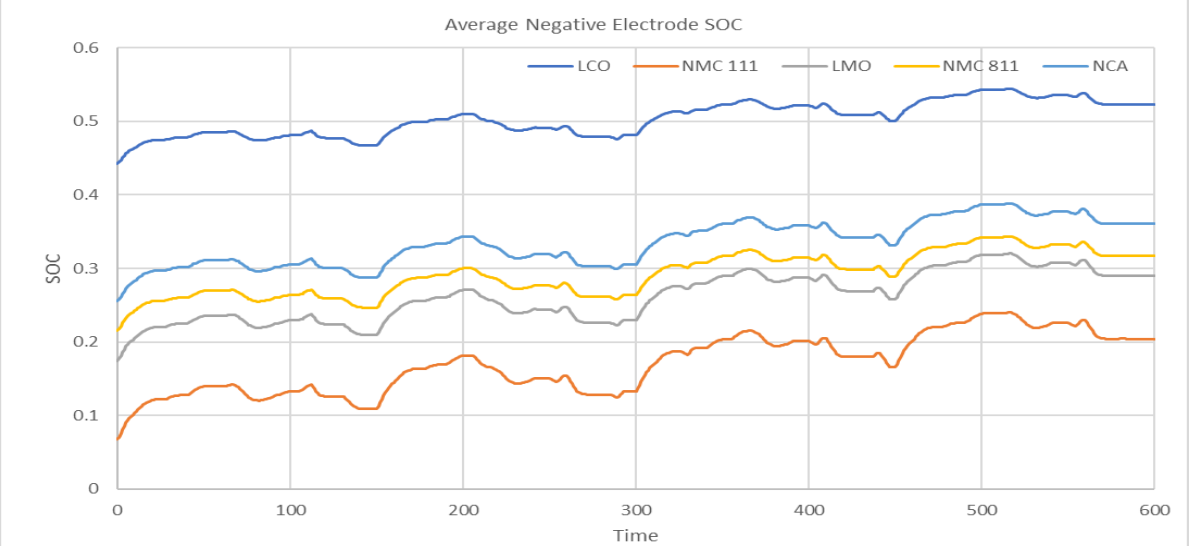

Figure 7: Comparison of Average negative electrode SOC with all the cell materials.

6. Cell Currents: The analysis in the figure 8 revealed that NMC 111 exhibited the highest cell currents among all cell materials, while LMO exhibited the lowest. Cell currents play a crucial role in determining the power output and charging capabilities of a battery. The higher cell currents observed in NMC 111 indicate its suitability for applications requiring high-power output and fast-charging capabilities.

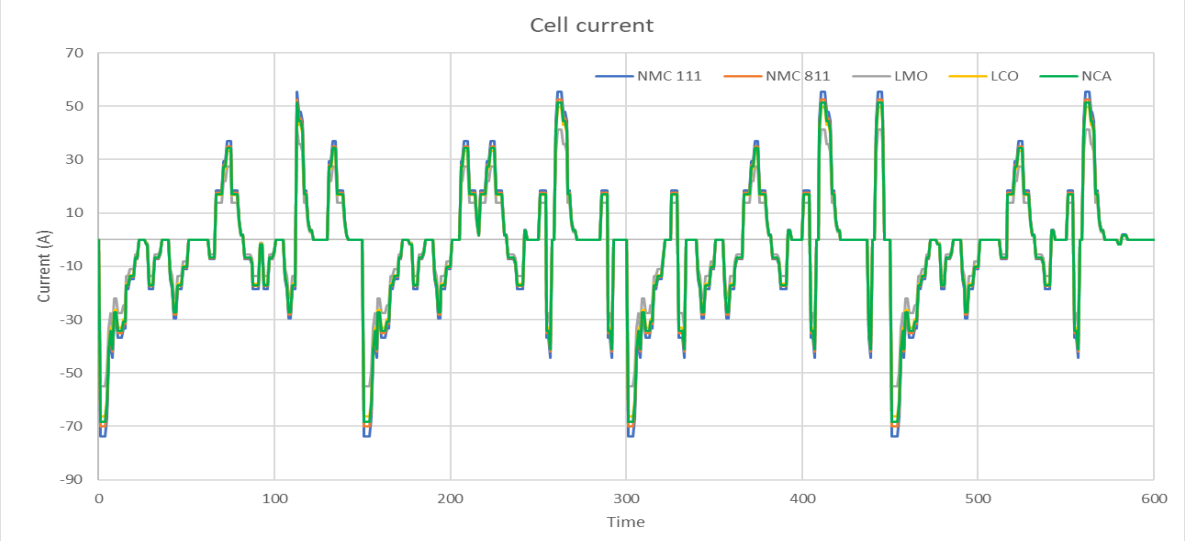

Figure 8: Comparison of cell currents with all the cell materials.

5. Discussion

The electrochemical model of 1-D lithium-ion cells incorporating different materials for simulating drive cycle scenarios is developed within the COMSOL Multiphysics Simulation Software. This model is employed to scrutinize various cell characteristics pertinent to battery performance under different operating conditions. The characteristics investigated encompass aspects such as voltage profiles, current profiles, polarization, average electrodes SOC, Boundary electric potential, Cell soc for charge/discharge cycles.

In conclusion, the 1-D electrochemical model reveals that LCO material exhibits the highest Boundary Electric Potential, Cell Voltage, Polarization, and Positive Electrode SOC. While this results in high energy density, increased power output, and improved efficiency, it also poses potential performance issues, safety hazards, and reduced lifespan. Despite these drawbacks, LCO remains suitable for various applications, including Electric Vehicles, Grid Energy Storage, Portable Electronics, Renewable Energy Systems, Aerospace, and Aviation. These applications benefit from LCO's characteristics, especially in terms of performance, efficiency, and reliability across diverse operational environments.

On the other hand, NMC 111 demonstrates high currents among all simulated cell materials, offering advantages in charging speed, power output, and application flexibility. However, these benefits come with drawbacks such as voltage drop, reduced efficiency, capacity loss, and accelerated degradation. Nevertheless, NMC 111 remains suitable for applications including electric vehicles, telecommunications, medical devices, aerospace, and renewable energy integration.

To mitigate the drawbacks associated with the highest Boundary Electric Potential, Cell Voltage, Polarization, and currents of LCO and NMC 111, the use of LMO material is suggested. LMO exhibits the lowest Boundary Electric Potential, Cell Voltage, Polarization, Positive Electrode SOC, and produces low currents. This provides a balance between performance and safety, making it a viable alternative for applications where mitigating these drawbacks is essential.

In summary, understanding the characteristics and trade-offs of different lithium-ion battery materials is crucial for optimizing performance, efficiency, and reliability in various applications. Each material offers unique advantages and drawbacks, and careful consideration of these factors is necessary to meet specific application requirements while ensuring safety and longevity.

Refrences

[1] L. Wu, Z. Lyu, Z. Huang, C. Zhang, and C. Wei, "Physics-based battery SOC estimation methods: Recent advances and future perspectives," Journal of Energy Chemistry, vol. 89, pp. 27–40, Feb. 2024, doi: 10.1016/j.jechem.2023.09.045.

[2] "Theory for Lithium-ion battery interface," doc.Comsol.com. https://doc.comsol.com/6.2/docserver/#!/com.comsol.help.battery/battery_ug_electrochem_battery.06.56.html (accessed Mar. 07, 2023).

[3] J. Tang, "COMSOL Simulation of the Storage Life of Zinc-silver Reserve Battery," Journal of Physics: Conference Series, vol. 2584, no. 1, p. 012001, Sep. 2023, doi: 10.1088/1742-6596/2584/1/012001.

[4] Y. Ghoulam et al., "Lithium-Ion Battery Parameter Identification for Hybrid and Electric Vehicles Using Drive Cycle Data," Energies, vol. 15, no. 11, p. 4005, May 2022, doi: 10.3390/en15114005.

[5] A. Li and S. L. Butler, "Forward modeling of magnetotellurics using Comsol Multiphysics," Applied Computing and Geosciences, vol. 12, p. 100073, Dec. 2021, doi: 10.1016/j.acags.2021.100073.

[6] "Comsol," IEEE Microwave Magazine, vol. 22, no. 11, pp. C4–C4, Nov. 2021, doi: 10.1109/mmm.2021.3111354. [7] J. Guo, Q. Guo, J. Liu, and H. Wang, "The Polarization and Heat Generation Characteristics of Lithium-Ion Battery with Electric–Thermal Coupled Modeling," Batteries, vol. 9, no. 11, p. 529, Oct. 2023, doi: 10.3390/batteries9110529.

[7] V. Goel and K. Thornton, "Enabling the electrochemical simulation of Li-ion battery electrodes with anisotropic tortuosity in COMSOL Multiphysics®," MethodsX, vol. 8, p. 101425, 2021, doi: 10.1016/j.mex.2021.101425.

[8] Y. Zhang, Y. Shang, N. Cui, and C. Zhang, "Parameters Identification and Sensitive Characteristics Analysis for Lithium-Ion Batteries of Electric Vehicles," Energies, vol. 11, no. 1, p. 19, Dec. 2017, doi: 10.3390/en11010019.

[9] 封琼, "Application Research of Comsol Multiphysics on Corrosion Protection," Hans Journal of Chemical Engineering and Technology, vol. 06, no. 03, pp. 33–42, 2016, doi: 10.12677/hjcet.2016.63005.

[10] N. Xue, W. Du, J. R. R. A. Martins, and W. Shyy, "Lithium-Ion Batteries: Thermomechanics, Performance, and Design Optimization," Handbook of Clean Energy Systems, pp. 1–16, Jul. 2015, doi: 10.1002/9781118991978.hces225.

[11] M. OCILKA and D. KOVÁČ, "SIMULATION MODEL OF INDUCTION HEATING IN COMSOL MULTIPHYSICS," Acta Electrotechnica et Informatica, vol. 15, no. 1, pp. 29–33, Mar. 2015, doi: 10.15546/aeei-2015-0005.

[12] H. He, R. Xiong, H. Guo, and S. Li, "Comparison study on the battery models used for the energy management of batteries in electric vehicles," Energy Conversion and Management, vol. 64, pp. 113–121, Dec. 2012, doi: 10.1016/j.enconman.2012.04.014.

[13] N. Watrin, H. Ostermann, B. Blunier, and A. Miraoui, "Multiphysical Lithium-Based Battery Model for Use in State-of-Charge Determination," IEEE Transactions on Vehicular Technology, vol. 61, no. 8, pp. 3420–3429, Oct. 2012, doi: 10.1109/tvt.2012.2205169.

[14] H. He, R. Xiong, and J. Fan, "Evaluation of Lithium-Ion Battery Equivalent Circuit Models for State of Charge Estimation by an Experimental Approach," Energies, vol. 4, no. 4, pp. 582–598, Mar. 2011, doi: 10.3390/en4040582.

[15] R. Xiong, H. He, H. Guo, and Y. Ding, "Modeling for Lithium-Ion Battery used in Electric Vehicles," Procedia Engineering, vol. 15, pp. 2869–2874, 2011, doi: 10.1016/j.proeng.2011.08.540.

[16] Ehsani, M.; Gao, Y.; Gay, S.E.; Emadi, A. Modern Electric, Hybrid Electric, and Fuel Cell Vehicles: Fundamentals, Theory, and Design; CRC Press: Boca Raton, FL, USA, 2018. [Google Scholar]

[17] Watrin, N.; Roche, R.; Ostermann, H.; Blunier, B.; Miraoui, A. Multiphysical lithium-based battery model for use in state-of-charge determination. IEEE Trans. Veh. Technol. 2012, 61, 3420–3429. [Google Scholar] [CrossRef]

[18] Mesbahi, T. Influence des Stratégies de Gestion d'une Source Hybride de Véhicule Électrique sur Son Dimensionnement et Sa Durée De Vie Par Intégration d'un Modèle Multi-Physique. Ph.D. Thesis, University Centrale Lille, Villeneuve-d'Ascq, France, 2017. [Google Scholar]

[19] MHannan, A.; Hoque, M.M.; Hussain, A.; Yusof, Y.; Ker, P.J. State-of-the-Art and Energy Management System of Lithium- Ion Batteries in Electric Vehicle Applications Issues and Recommendations. IEEE Access 2018, 6, 19362–19378. [Google Scholar]

[20] Dubray, A. Adaptation des Lois de gestion D'énergie des Véhicules Hybrides Suivant le Profil de Mission Suivi. Ph.D. Thesis, Institut National Polytechnique de Grenoble—INPG, Grenoble, France, 2002. [Google Scholar]

[21] Watrin, N.; Bouquain, D.; Blunier, B.; Miraoui, A. Multiphysical lithium-based battery pack modeling for simulation purposes. In Proceedings of the 2011 IEEE Vehicle Power and Propulsion Conference, Chicago, IL, USA, 6–9 September 2011; pp. 1–5. [Google Scholar]

[22] Nikolian, A.; Firouz, Y.; Gopalakrishnan, R.; Timmermans, J.-M.; Omar, N.; Van den Bossche, P.; Van Mierlo, J. Lithium Ion Batteries—Development of Advanced Electrical Equivalent Circuit Models for Nickel Manganese Cobalt Lithium-Ion. Energies 2016, 9, 360. [Google Scholar] [CrossRef]

[23] Smekens, J.; Omar, N.; Hubin, A.; van Mierlo, J.; van den Bossche, P. Optimization of Li-ion batteries through modelling techniques. World Electr. Veh. J. 2015, 7, 52–58. [Google Scholar] [CrossRef] [Green Version]

[24] Tatsumi, K. Aspects of Technology Developments of Lithium and Lithium-ion Batteries for Vehicle Applications in National R&D Projects of Japan. J. Asian Electr. Veh. 2010, 8, 1415–1418. [Google Scholar]

[25] Yasser, G.; Theophile, P.; Tedjani, M.; Sylvain, D. Modeling, Identification and Simulation of Hybrid Battery/Supercapacitor Storage System Used in Vehicular Applications. In Proceedings of the 2019 6th International Conference on Electric Vehicular Technology (ICEVT), Bali, Indonesia, 18–21 November 2019; pp. 156–162. [Google Scholar]